Bollettino di Geofisica Teorica ed Applicata Vol. 53, n. 4, pp. 509-522; December 2012
DOI 10.4430/bgta0073

Borehole microseismic in deep live oil wells: an example

L. Barzaghi and M.F. Ferulano

Eni Exploration & Production Division, San Donato Milanese (MI), Italy

(Received: March 25, 2011; accepted: November 28, 2011)

ABSTRACT Passive seismic monitoring of development activities at reservoir level is a challenging activity. Seismic signals of very low energy are emitted, and only few are detectable from surface tools. To improve quantity and quality of detected signals, the sensors must be deployed deep in the Earth, close to the sources. The instrumentation of a well is costly from both the economic and the technical point of view but can give useful information for the understanding of the reservoir dynamics. A dedicated well to install the microseismic sensors is rarely available, so that, the possibility to use a live well is very attractive. The field test performed by Eni successfully demonstrated the possibility to record microseismic events during well activity, with a smooth integration into well completion. The clear correlation between well operations and microseismic events helped to improve the reservoir model close to the well.

Key words: microseismic monitoring, reservoir.

1. Introduction

The development of borehole microseismic roots back to the 1970s when, after the "petroleum shocks", the interest for alternative energy sources developed. In those years, a renewed attention was given to geothermics. In order to improve the applicability of the technology, the so called Hot Dry Rock (HDR) projects were launched in various sites around the world. Normally, the geothermal heat in deep layers is made available by steam or hot water already in place underground. But if there is no fluid, in order to be able to extract heat from hot rocks, water is pumped down deep, where it is heated and brought up to the surface again. The water injection can also be used to fracture rocks and to improve the fluid circulation. All these activities need to be carefully controlled. So, a strong effort on monitoring was set in place during the HDR projects and the importance of the passive seismic monitoring conducted into deep boreholes emerged (Niitsuma *et al*., 1999). Theoretical studies as well as field techniques were developed, and they still represent the background of the today applications in the oil industry.

Diffusion of borehole microseismic in the petroleum industry began only in the late 1990s, when the successful applications on Ekofisk (Maxwell *et al*., 1998) and Valhall (Dyer *et al*., 1999) fields demonstrated the potentiality of the technology.

Since those early installations, borehole microseismic monitoring developed constantly. The most successful example is given by the hundreds of microseismic monitorings yearly performed during the hydraulic fracturing treatments. The monitoring system is installed into an observer well, close to the injector well, for the duration of the treatment (from some hours to few days) and then retrieved. Such kind of installations makes use of the standard wireline tools normally used for active borehole seismic. Many times it is not possible to use observation wells, due to the distance

from the treatment well or for technical/economical reasons. In such situations, it has been proved in recent years (see for instance Chambers *et al*., 2010; Eisner *et al*., 2010) the possibility to monitor the microseismic activity during hydraulic fracturing by dense surface arrays of standard seismic sensors.

If the interest is for long term monitoring, it is necessary to install a permanent system inside the well.

The best and easiest solution would be to instrument a dedicated well, which guarantees the best Signal/Noise Ratio (SNR) for the recordings. One successful example of the previous approach is the instrumentation of the Yibal field in Oman (Jones *et al*., 2004; Al-Anboori *et al*., 2006). Unfortunately, this option is rarely available, both for technical and economic reasons. In order to overcome the above constraints, it would be necessary to instrument an active well. It could be done with the sensors behind casing and formation, without interference with well operations and a good SNR. Unluckily, this solution is highly risky for the integrity of the system during running down hole to the depth of installation. In recent years some technology providers developed a new generation of tools which can be installed into live wells, inside casing, as part of the completion (Wilson *et al*., 2004; Hornby *et al*., 2005; Maver *et al*., 2009). A good decoupling from fluid flow noise is possible and a SNR as good as the one of sensors behind casing can be obtained. Moreover, the system can be retrieved with the completion in case a work over is planned.

2. Rationale for borehole microseismic monitoring

During the exploitation phase of a reservoir, the stress field can be modified by hydrocarbon production or fluid injection. Subsurface structures could react to the stress changes, depending on rock characteristics, with micro-cracks inside or close to the reservoir. These micro-cracks can be studied with the techniques developed in seismology, being the low energy released the main difference.

Relying only on passive sources, the major problem of the microseismic technique is the lack of control on the source. The number of the recorded events, if they do exist, depends on the energy released in the micro-fracture process and on the distance between the source and the receiver. So, in order to get the number of events useful for the detailed analysis required in reservoir monitoring, it is necessary to push the magnitude of recorded events possibly down in the range -3 ÷ -1. The energy associated to such events is so low that none or few of them are detectable from surface tools, placed some kilometres above the reservoirs. Moreover, precise localizations are necessary at reservoir scale. To improve the quantity of detected signals and the precision of the locations, the sensors must be deployed down hole close to the sources, near or inside the area to be studied. An example of the above is presented in Fig. 1 for the Ekofisk installation (Maxwell *et al*., 1998), where the number of events is plotted versus the distance from the borehole microseismic string: almost no events are recorded beyond 1000 m and the majority is within 800 m. So, because the installation depth of the microseismic string is about 3000 m b.s.l., it is clear that none of the signals emitted by those events would have been recorded by a surface tool.

The evolution of the technology nowadays makes possible to install the microseismic sensors into active well. This option is very attractive for the geophysicists as it gives a wide flexibility in choosing the well whose position in the field is more appropriate for the monitoring goals.

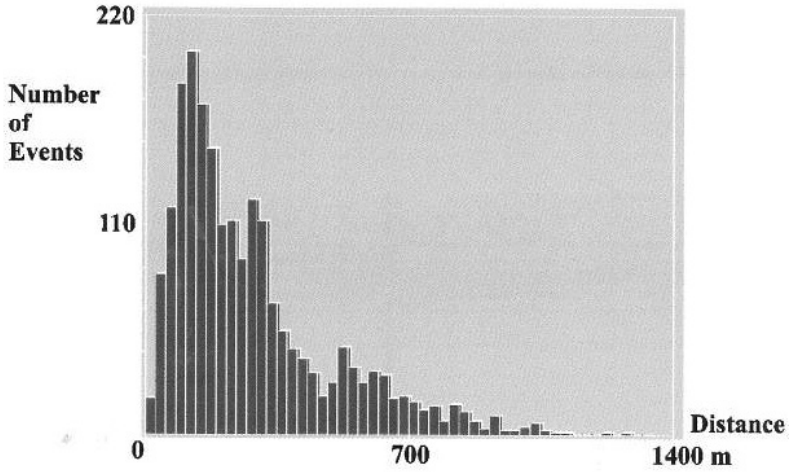

Fig. 1 - Histogram of the number of microseismic events vs. distance from borehole microseismic string at Ekofisk (from Maxwell *et al*., 1998).

The microseismic system to be installed into a live well must fulfil the following constraints:

- to allow the measurement in a flowing well, it must be insensitive to flow noise;
- no production/injection stops during measurements;
- no restriction in the flow pass to allow full efficiency of the well;
- design life about 10 years because there is no possibility to retrieve the system for repairing;
- must be retrievable in order not to hamper the possible work over of the well;
- must be placed between production tubing and casing, to get safe deployment of tools;
- possibility to be installed into highly deviated or horizontal wells, which are the most common during field development;
- must be integrated into the well completion with minor modifications to the original design.

With the above characteristics, the microseismic system meets the needs of the drilling and completion engineers and overcomes the resistance of the reservoir engineers, interested in not to loosing production. At the same time, it realizes an effective monitoring, recording seismic signals with quality comparable to that of the sensors placed behind the casing.

In August 2007, Eni Exploration & Production Division installed a borehole microseismic string into an oil producer well, drilled in a complex geological context, with reservoir made by fractured carbonates at an average depth of 4000 m below ground level. The chosen tool, produced by a major oil service company, is shown in Fig. 2. The seismic sensors are placed in a cartridge mounted on shuttle which is a C-shaped single piece of iron, slightly larger than the casing size within which it must be deployed. During the run-in-hole phase, the shuttle is held compressed against the tubing by a fork. Once the tubing string is in place, the fork is retrieved by the action of a hydraulic piston and the shuttle is then released from the tubing. When released, it never reaches its full relaxed state and is physically constrained by the casing. The clamping force, that imparts to the inside of the casing, is quantified as part of the design process. The shuttle and the sensors it contains no longer touch the tubing and there is no direct mechanical noise path from the tubing to the sensors.

The tool contains four, high gain, geophones assembled in a tetrahedral configuration. The 4 components can be combined to recover the 3D particle motion but has the advantage of redundancy over the standard 3 orthogonal components: if one geophone fails, it is always possible

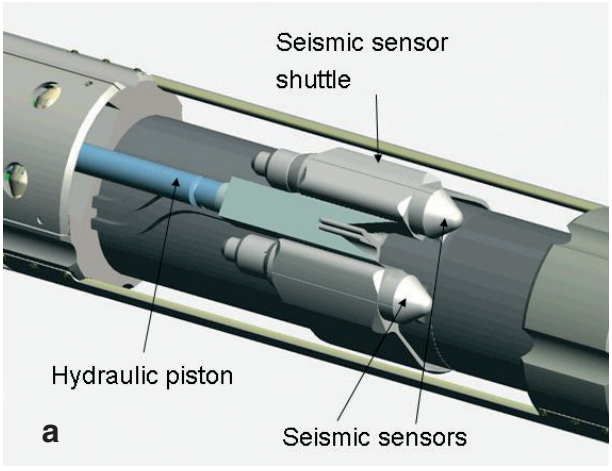

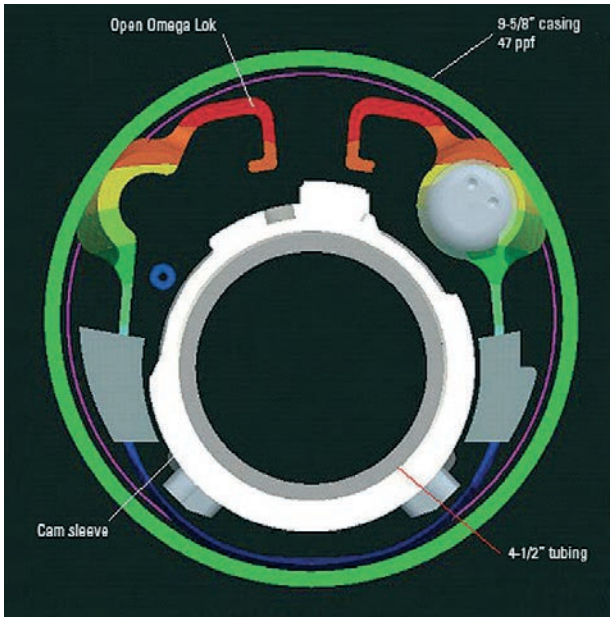

Fig. 2 - a) The scheme of the microseismic tool with description of the main elements; b) the sketch shows the C-shaped shuttle in a semi-relaxed stated clamping against the casing and decoupled from the inner tube (from Maver *et al*., 2009).

to recover the complete wavefield from the remaining 3 sensors. Moreover, when combining the 4 signals to get the 3 orthogonal components, a coherency measure is derived to get a quality control of the data acquisition (Jones and Asanuma, 2004) and it is plotted together with the 3 sensor traces (coherency is a measure of the similarity between two or more signals in the same frequency band: it is 1 for nearly identical signals and 0 for uncorrelated signals).

The downhole equipment is fully passive electro-mechanical, to avoid weak electronic devices in a hostile and not accessible environment. The analog signals from the sensors are delivered up to the surface, where the acquisition system provides the analog to digital conversion, time stamp, storage and pre-processing.

The system requires 2 cables, an electrical one to deliver signals and a hydraulic one to open the sensors shuttle. They must pass through the wellhead and go downhole. Therefore, completion

engineers must be made aware of the necessity for the two passages in the wellhead equipment.

3. Field installation and processing details

The original plan was to install a string of 4 levels and to keep it permanently all along the well life. Unfortunately, the installation suffered some technical problems due to well activities. First, good cementation of the casing, in the depth section of the well where the space between casing and tubing was enough to host the tools, was limited and located far above the reservoir. So, it has been possible to install only 2 levels, at depths of 2809 and 2924 m below ground level, in the deviated section of the well and about 1 km above the reservoir. Second, in order to improve the production performances, the well was de-completed to install a downhole pump. The string had to be retrieved and the presence of the pump prevented to install it again. The retrieval procedure worked correctly and the tools resulted fully operative after the tests in laboratory and available for a new installation. For all these reasons the string was made by 2 levels and remained in place only for 2 months with continuous recording.

A total of 5 cables, 2 for the microseismic string and 3 for other well equipment, had to pass through the wellhead and their integration had to be designed several months before the installation in order to guarantee the safe activity of the well.

At the end of the deployment, the orientation of the sensors in the 2 tools was unknown, because the tubing pipe rotates during the descent into the well. The tools have no equipment on board to get a direct measure of the orientations. The orientations could be derived from artificial shots on the surface on different azimuths. Analysis of the arrival directions allows to derive the orientation of the sensors. In the case of our installation, it has not been possible to use the surface shots due to timing of the operations and problems with permits to be issued by the authorities. Therefore, the orientations have been derived by analysing the arrival direction of the signals from regional earthquakes. After transforming the four-component data to three-components, total of 5 regional events, recorded also by the downhole tools, have been examined and the rotation matrixes for the 2 tools have been derived.

The surface acquisition system converted analog signals to digital with a sampling frequency of 2 kHz, time stamped the data with GPS reference, stored the data on removable hard disks and managed communications for remote connections. The limited portion of a satellite channel, allowed to check the status and the parameters of the system, but to download only very short data files. Data have been retrieved manually on a monthly basis. Another task performed by the acquisition system is to survey the background noise at the site (i.e., downhole). The RMS value of the signal recorded has been computed continuously, after the removal of the electrical noise with a filter, producing one derived measurement every 10 seconds. The results are plotted on Fig. 3 (the plot colour alternates each day between red and blue): during the first month of acquisition (Fig. 3a) and for the second month (Fig. 3b). On top of these values an amplitude range (in yellow) is shown for comparison with the signal of the recorded microseismic events. Very high values of RMS correspond to disturbances occurring in the well or at the rig site during the stimulation period (A circle) or just before the pull out of the tool (B circle).

A number of different trigger algorithms has been used to extract triggered events from the continuous data sets. They involved several iterations to identify the best combination of filters and

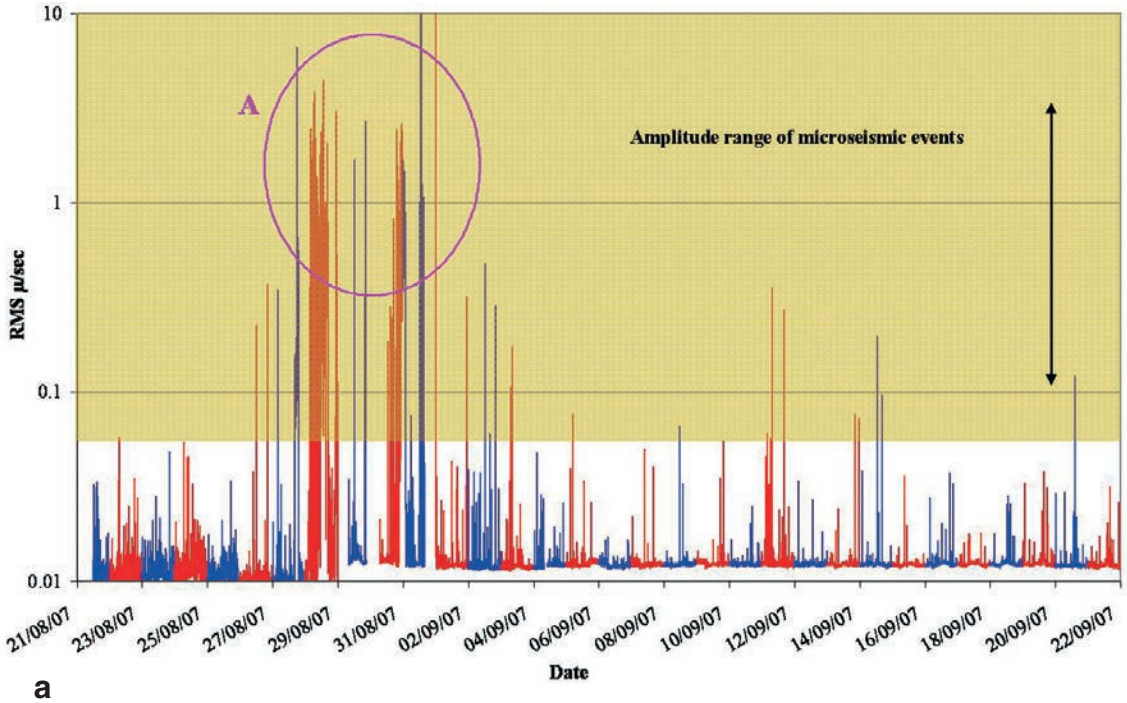

a

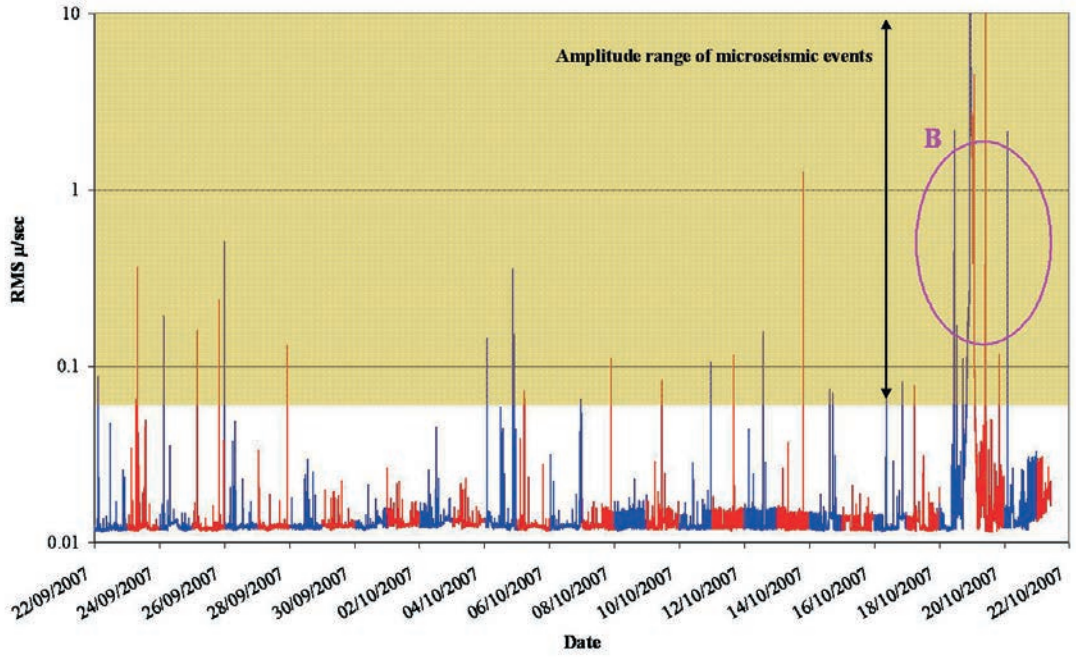

b

Fig. 3 - RMS of the signal recorded on vertical component of lower tool during the first month of acquisition (above) and the second month (below).

parameters to extract the highest proportion of events. The raw data from the first day have been examined manually to check the efficiency of the trigger settings. The same settings have been applied to the entire set of data. Among the 8 available channels, 4 channels mixed from the two tools have been included within the trigger logic, because the signal to noise ratio seemed larger on these channels than on the others. Of these four channels, only three had to exceed the threshold in order for the trigger to be satisfied. Before applying the trigger logic, the data have been frequency filtered (filter pass band was 20 - 100 Hz) and then an STA/LTA (Short Time Average to Long Time Average ratio) algorithm applied. The number of triggers varied greatly from day to day. During the stimulation period, with the increase of the rig activity, the number of triggers reached 700, while during more quiet periods only 3 or 4 triggers per day have been observed.

Once the raw data have been processed through the triggering software, triggers have been examined to identify detected events. To do this, some criteria have been followed. The most important considers that the reservoir was below the string; therefore, we were interested in the study of the events whose signals reached the bottom tool first and then the top tool. Another criterion is the presence of two phases to each event with an amplitude difference between them. Fig. 4 shows the traces associated to 2 microseismic events at different distance from the tools: about 1.3 km away (Fig. 4a) and about 2.5 km (Fig. 4b). For both events P and S phases are easy to detect, but the SNR is different. This is suggested also by the different behaviour of the coherency traces, especially after the P phase arrival.

The frequency analysis for 2 microseismic events is presented in Fig. 5. In Fig. 5a, the result for the event in Fig. 4a shows that the energy is up to 130 Hz for both P and S waves, but S waves have energy mostly at frequencies around 30-50 Hz. For a distant event (Fig. 5b) the energy content is reduced below 60 Hz and S waves are mainly in the band 10-30 Hz.

Log data from several wells in the area were available and have been used to build a 1D velocity model, approximating the subsurface with horizontal homogeneous layers. A Vertical Seismic Profile had been acquired in the instrumented well, and an inversion procedure has been performed to further constrain P and S velocity values. Different velocity models have been tested and at the end a smooth model have been used to avoid the strong velocity contrasts which trap the hypocentres on velocity boundaries. This location artefact is enhanced by the limited geometry of the microseismic string.

For each identified microseismic event, P-wave and S-wave arrival times have been picked on both levels where the phase could be identified above the background noise. In addition, hodograms have been computed wherever possible. The location method used in this analysis is essentially Geiger's method (Bornam, 2002), modified to use the polarisation information. Geiger's method is an iterative method based on linearization of the travel time functions by Taylor expansion, assuming a trial location close enough to the real hypocentre. In this hypothesis, the travel time residuals at the trial location are linear function of the correction to make in hypocentral distance. Travel times are computed by ray tracing through the velocity model.

4. Results and interpretation

During the monitoring period 180 microseismic events have been detected and 103 located. Fig. 6 shows the cumulative number of events detected and the distance of the located events versus time. Distance is computed from the centre of the string, i.e., mid point between the 2 tools.

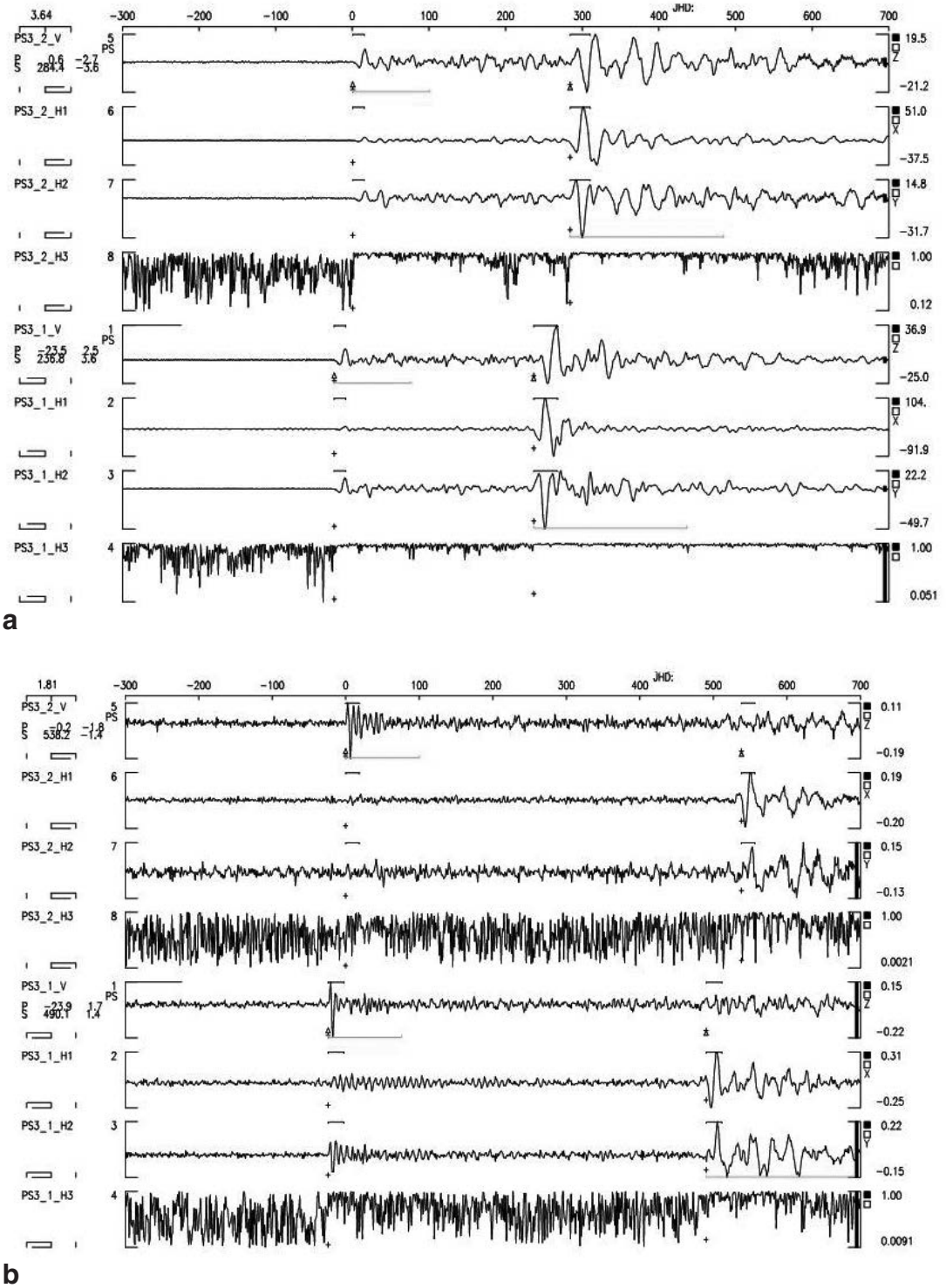

Fig. 4 - Traces of microseismic events after transformation from 4 to 3 components and rotation. Traces 1-4 lower tool, traces 5-8 upper tool. Traces 1 and 5 are vertical. Traces 2 and 6 are east. Traces 3 and 7 are north. Traces 4 and 8 are coherency data computed during transformation. a) is an event close to the tools; b) is a more distant event.

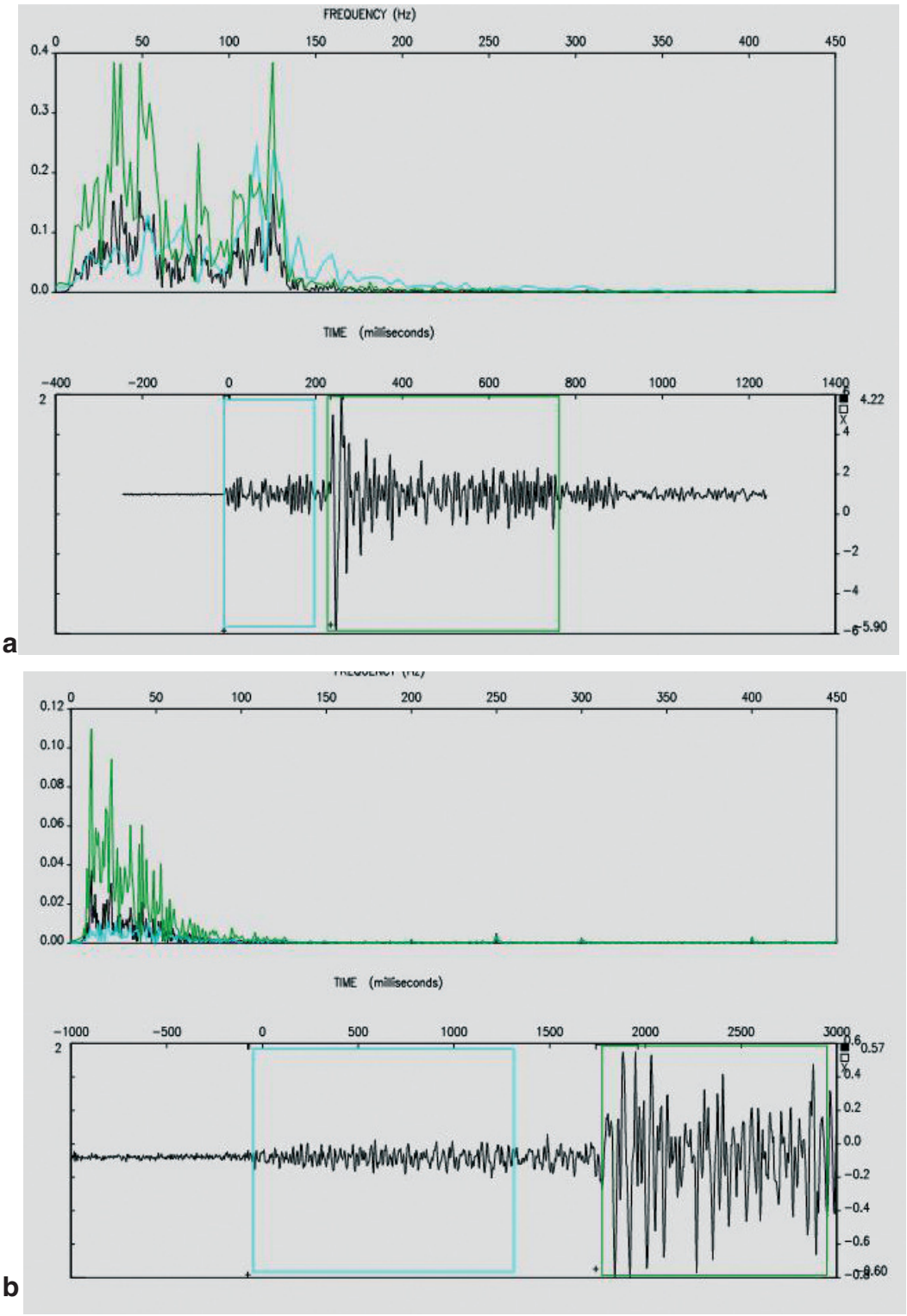

Fig. 5 - Frequency analysis of microseismic events. Green curve is S wave spectrum, blue curve is P wave spectrum, black curve spectrum for complete event (different scale). Rectangles represent the P wave (blue) and S wave (green) arrivals. a) analysis for the event in Fig. 4a; b) for an event at a distance of about 9 km.

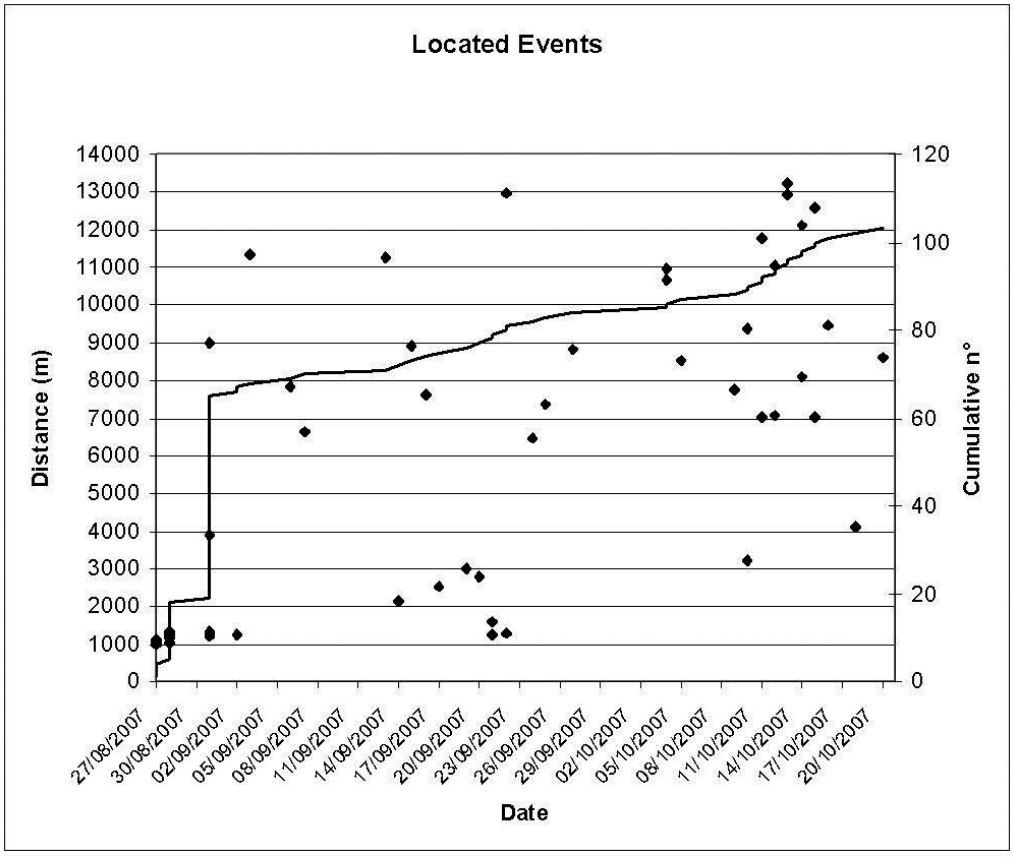

Fig. 6 - Cumulative number of located events (continuous curve) and events distance (diamonds) versus time.

Distance range is 1 ÷ 13 km. Events located closer to the well, below 2 km, occur mostly during the first week of monitoring. After that, there are mostly far away events (above 6 km), not directly related to the activity of the well, but to the natural seismicity of the area. Fig. 7 presents the distribution of the moment magnitude versus distance. Magnitude values span the range -1.5 ÷ 0.9. The dashed curve identifies the detection limit of the borehole microseismic string. Closer events occurred during the noisiest period, so it is probable that weaker signals have been lost into the noise. From that, it is possible to extrapolate a magnitude -2 in case of events close to the string. The above results are consistent with the position of the string: the reservoir, which is the potentially active area, is more than 1 km distant from the string, therefore, we did not expect to detect closer events.

The analysis focused on the group of events in the first week of monitoring, because they are related to well operations. A total of 57 events took place between 1 and 1.5 km from the string and had a clear time correlation with the activities associated to well acidification. Acidification has been carried out to prepare the well for production and to improve its performances. It consisted of 3 phases, applied to the open hole section of the well: first, solvent injection to clean the well from drilling residuals; second, acid injection to complete the cleaning and place acid throughout

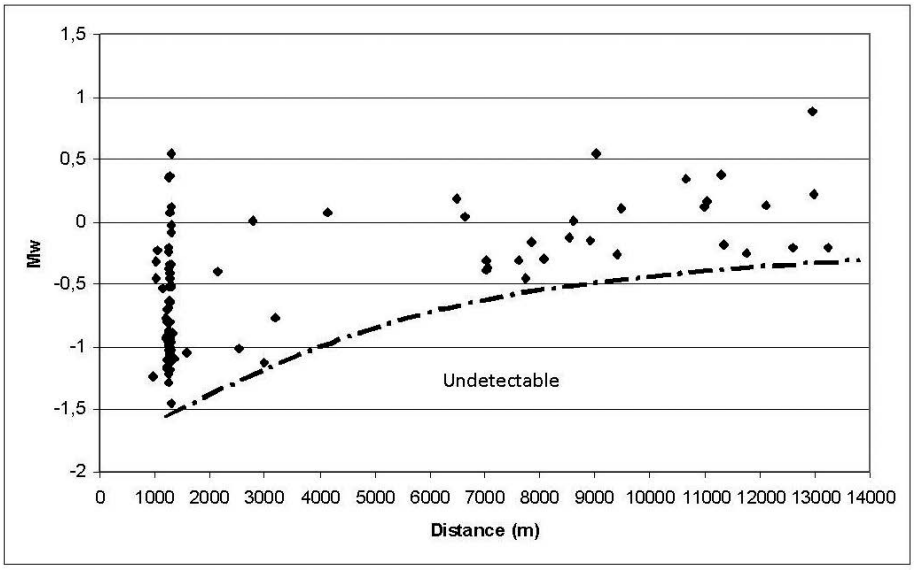

Fig. 7 - Moment magnitude of the 103 located events versus distance. Dashed curve identifies the detection limit of the microseismic system.

production interval; third, pressurised acid injection to penetrate into the formation. In Fig. 8 the temporal evolution of seismic events, fluid flow rate and pressure in the well are plotted together to show the correlation between seismic activity and the well operations: seismic events occurred when pressure and/or flow rate increase. During solvent injection, lasting about 7 hours, 4 seismic events have occurred. 13 events have taken place during the first acid injection of 6 hours. Then, 39 events have been associated to the second acid and the majority of them have occurred in a short period of 30 minutes, when both pressure and flow rate increased.

Hypocentre location is shown in Fig. 9, with different colours for the 3 phases of acid treatment: red for solvent, green for first acid and yellow for second acid. The microseismic events group into two clusters to map out the existence of two possible faults: strikes are about 310° E, one dipping to the SSW and the other to the NNE. The locations contained within these features suffer from a significant sensitivity to hodograms used to constrain each location. The limitations of the network geometry, which results in a poor transverse constraint, induce a distortion of the true distribution of the microseismic event population and likely exaggerate the extent of the features.

The following interpretation of the results has been proposed: due to the presence of the fault dipping NNE, some proportion of the solvent exited the well at the beginning of the open hole section, close to the casing shoe. Then, part of the acid flowed into the discontinuity and, during the final phase, extended into the 2 faults. Therefore, the well was neither fully cleaned by the solvent nor fully stimulated by the acid, which resulted in low production performances.

Finally, microseismic locations have been compared with the reservoir model. A correspondence has been found between a seismic fault near wellbore and the microseismic feature dipping NNE. Other seismic faults, crossed forward by the borehole, remained "silent" during the stimulation. The microseismic feature dipping SSW maps a permeable fracture which was not observed in any other

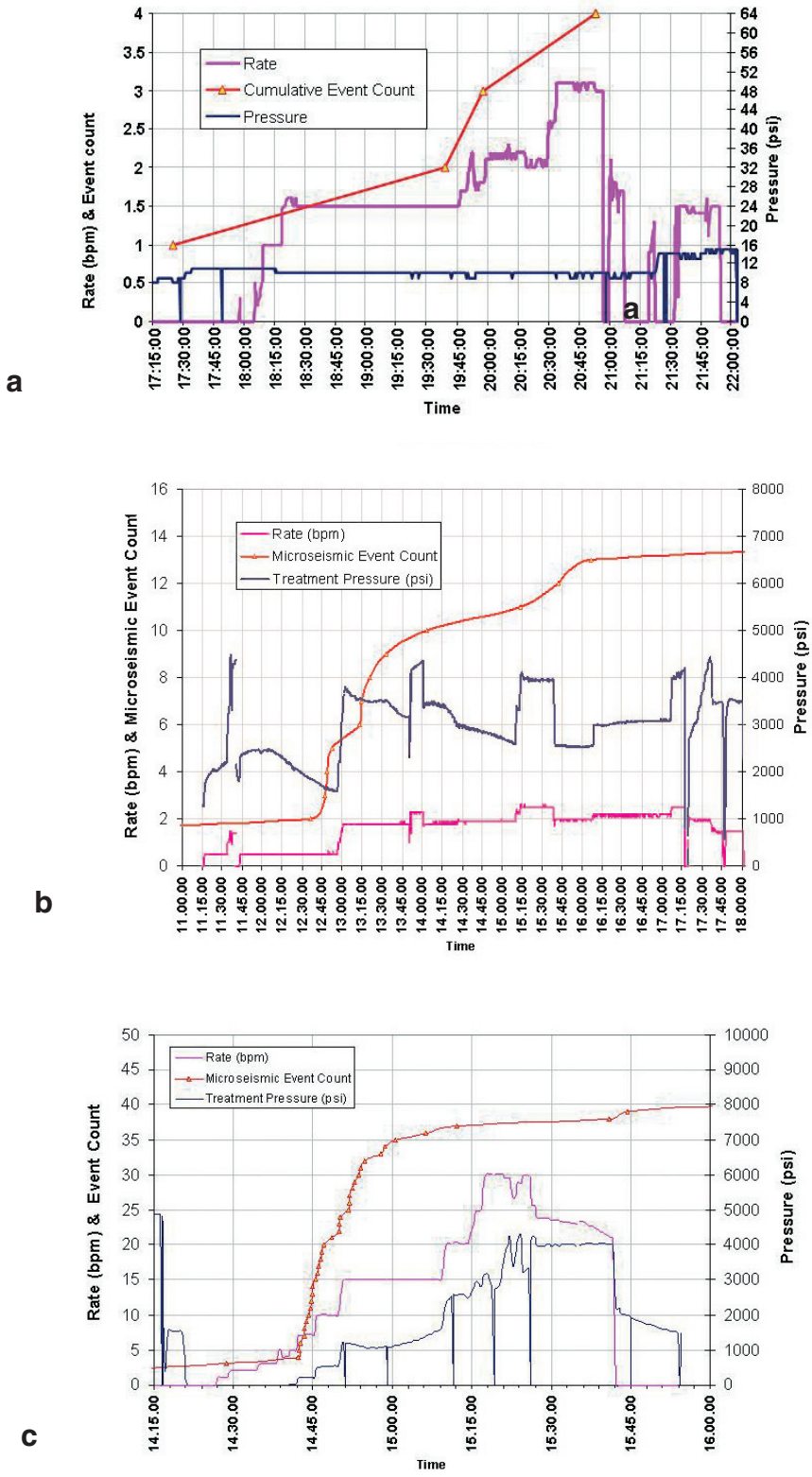

Fig. 8 - Injection rate, well head pressure and cumulative event count for the three phases of acid stimulation.

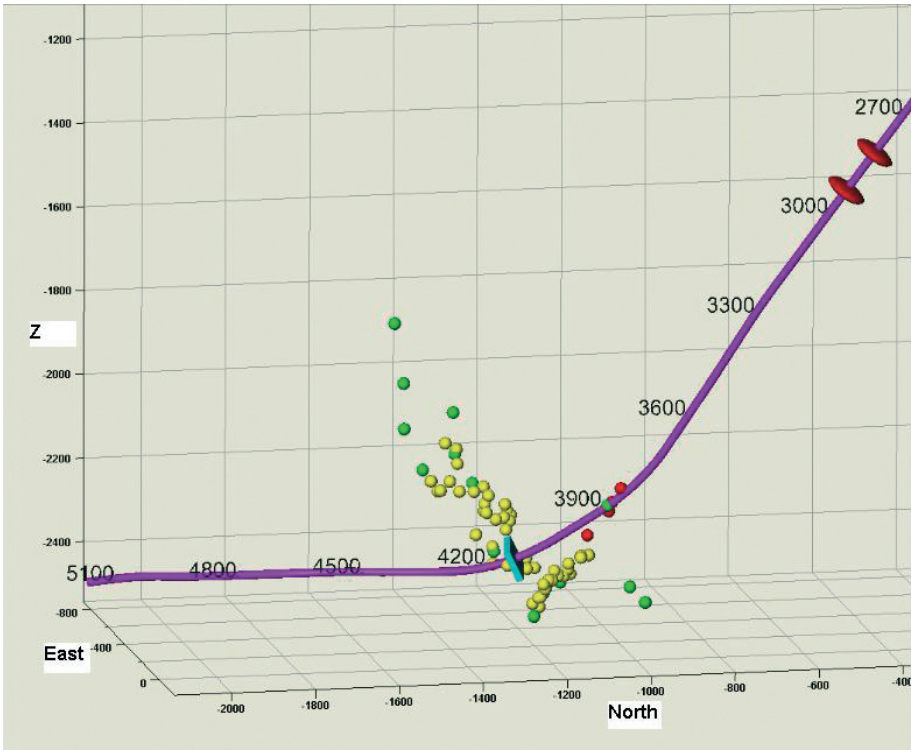

Fig. 9 - Plot of events during acidification. Red dots are events during solvent injection, green dots are events of the first acid phase and yellow dots are the events of the pressurised acid. Not scaled for magnitude. Purple line is the well track. Red disks indicate the position of the microseismic tools. Blue rectangle marks the beginning of the open hole section. Distances in metres.

data. This information has been included into the fracture network model which is an important item of the revised static reservoir model.

5. Conclusions

The field test successfully demonstrated, beyond the technical limitations suffered, the possibility to record useful microseismic data, with only minor modifications to the completion program and the activities of the well. Even during extremely invasive operations, like the acid treatment, the microseismic equipment has been completely "hidden", and continued to record data efficiently, little affected by the noise in the well. It is important to emphasize the following topics:

- the low impact required for the integration of the tools into the completion of a live well;
- the successful recovery of the tools, still fully working. This task was not originally planned in the project as the string should have stayed permanently in the well;
- the possibility to continuously record reliable signals while the well is operating, with no stops required. Many of the recorded signals are easily recognized as microseismic events;
- the existence of a strong temporal correlation between groups of detected events and specific well operations (the acid treatment);

- the value added by microseismic information to the management of the well and their integration into the reservoir model in the area close to the well;
- the complete safety during the development of all the activities, run without any effect for the health of the human operators and the environment.

Acknowledgements. We would like to thank the management of Eni E&P Division for the support given during the project and the permission to publish the results. Many people in Eni E&P Division contributed to the success of the project: we thank our colleagues of the microseismic team for their help and collaboration throughout all the project; the colleagues of the drilling and completion department who helped us to manage the installation of the microseismic tools; the crews on the well site for the their help and assistance during installation and retrieval operations. This paper originated from a communication given by the authors at the 29th GNGTS congress held in Prato on October 26-28, 2010. The authors want to thank two anonymous reviewers for their suggestions.

REFERENCES

Al-Anboori A., Kendall M., Raymer D. and Jones R.; 2006: *Spatial variations in microseismic focal mechanisms, Yibal field, Oman.* In: Proc. 68th Conf. and Exhib., EAGE, Vienna, Austria, extended abstracts, A048.

Bornam P. (ed); 2002: *New manual of seismological observatory practice.* IASPEI, vol. 2, IS 11.1., 28 pp.

Chambers K., Kendall M., Brandsberg-Dahl S. and Rueda R.; 2010: *Testing the ability of surface arrays to monitor microseismic activity.* Geophys. Prospect. **58**, 821-830.

Dyer B.C., Jones R.H., Cowles J.F., Barkved O. and Folstad P.G.; 1999: *Microseismic survey of a North Sea reservoir*. World Oil, **220**, 74-78.

Eisner L., Williams-Stroud S., Hill A., Duncan P. and Thornton M.; 2010: *Beyond the dots in the box: microseismicity-constrained fracture models for reservoir simulation.* The Leading Edge, **29**, 326-333.

Hornby E.H., Bostick III F.X., Williams B.A., Lewis K.A. and Garossino P.G.; 2005: *Field test of a permanent in-well fiber-optic seismic system.* Geophysics, **70**, E11-E19.

Jones R.H. and Asanuma H.; 2004: *Optimal four geophone configuration, vector fidelity and long-term monitoring.* In: Proc. 66th Conf. and Exhib., EAGE, Paris, France, expanded abstracts, P294.

Jones R.H., Raymer D., Mueller G., Rynja H. and Maron K.; 2004: *Microseismic monitoring of the Yibal oilfield.* In: Proc. 66th Conf. and Exhib., EAGE, Paris, France, extended abstracts, A007.

Maver K.G., Boivineau A-S., Rinck U., Barzaghi L. and Ferulano F.; 2009: *Real time and continuous reservoir monitoring using microseismicity recorded in a live well*. First Break, **27**, 57-61.

Maxwell S.C., Young R.P., Bossu R., Jupe A.J. and Dangerfield J.; 1998: *Microseismic logging of the Ekofisk reservoir.* In: Proc. SPE/ISRM, Eurock98, Rock Mechanics in Petroleum Engineering, Trondheim, Norway, 47276, pp. 387-394.

Niitsuma H., Fehler M., Jones R., Wilson S., Albright J., Green A., Baria R., Hayashi K., Kaieda H., Tezuka K., Jupe A., Wallroth T., Cornet F., Asanuma H., Moriya H., Nagano K., Phillips S.W., Rutledge J., House L., Beauce A., Alde D. and Aster R.; 1999: *Current status of seismic and borehole measurements for HDR/HWR development.* Geothermics, **28**, 475-490.

Wilson S., Jones R., Raymer D. and Jaques P.; 2004: *Passive seismic makes sense for 4D reservoir monitoring.* First Break, **23**, 59-65.

Corresponding author: Lorenzo Barzaghi
Eni Exploration & Production Division
Via Emilia 1, 20097 San Donato Milanese, (Milano), Italy
Phone: +39 02 52063060; fax: +39 02 52061862; e-mail: lorenzo.barzaghi@eni.com